Brazilian Journal of Biometrics, **44**, 1–19 (2026)
doi:10.28951/bjb.v44i3.964

BRAZILIAN JOURNAL OF BIOMΣTRICS
ISSN:2764-5290

ARTICLE

Mark variogram of spatio-temporal point processes in the analysis of fire hotspots in Itapuã do Oeste, Brazilian Amazon

Rodrigo Ferreira de Abreu[⋆,1] and João Domingos Scalon[⋆,2]

[1]Federal Institute of Education, Science, and Technology of Southern Minas Gerais, Brazil
[2]Statistics Department, Federal University of Lavras, Brazil
[⋆]Corresponding author. Email: rodrigo.abreu@ifsuldeminas.edu.br; scalon@ufla.br

(Received: August 8, 2025; Revised: May 7, 2026; Accepted: May 22, 2026; Published: September 14, 2026)
Section Editor: Douglas Mateus da Silva

Abstract

Point processes are widely used statistical tools for analyzing spatial, temporal, or spatiotemporal patterns in several phenomena, such as crime occurrences, seismic events, plant species distribution, and fire hotspots. However, the analysis of these events requires distinguishing genuine spatiotemporal interaction structures from intensity trends in order to avoid misleading interpretations of clustering patterns. The objective of this study is to analyze the spatiotemporal behavior of fire hotspots in the Brazilian Amazon region, using the municipality of Itapuã do Oeste between 2018 and 2019 as a case study. Following an existing methodology, we apply the mark variogram, a technique traditionally used for marked point processes, to data from a spatiotemporal point process (STPP). The approach consists of decomposing the STPP into two marked point processes: one considering occurrence times as marks of spatial locations and the other considering spatial locations as marks of occurrence times, followed by fitting a Gaussian model. To improve the inferential interpretation of the method, we extend this approach by constructing simulation envelopes under both homogeneous (HPP) and non-homogeneous Poisson process (NHPP) null models. All analyses were performed in the R environment. The results revealed a spatial dependence structure for fire hotspots up to approximately 4 km. In the temporal domain, however, the observed clustering pattern was mainly associated with first-order intensity variation rather than true second-order dependence. Under the HPP null model, the empirical mark variogram lay significantly outside the simulation envelopes, suggesting apparent structural clustering. However, under the NHPP null model, the empirical function remained entirely within the envelope limits, indicating that the observed clustering behavior can be explained by non-homogeneous intensity patterns. These results demonstrate that incorporating non-homogeneous simulation envelopes into the analysis of spatiotemporal mark variograms improves inferential reliability by reducing false clustering interpretations. Consequently, the proposed approach provides a more robust framework for understanding fire dynamics and may support environmental monitoring and management strategies in critical ecosystems such as the Amazon rainforest.

Keywords: Mark variogram; Point process; Amazon; Hotspots.

1. Introduction

Many types of phenomena can be studied from the perspective of point processes, including seismic events (Ogata, 1998; Schoenberg, 2003; Vere-Jones & Deng, 1988), forest fires (Aragó *et al.,* 2016; Møller & Díaz-Avalos, 2010; Podur *et al.,* 2003; Turner, 2009), infection by a specific disease (Diggle, 2013; Lawson & Zhou, 2005; Perez *et al.,* 2004), location of plants of a particular species in a forest (Comas & Mateu, 2007; Penttinen *et al.,* 1992; Stoyan & Penttinen, 2000), galaxy clusters (Beisbart & Kerscher, 2000), crimes in a city (Gervini, 2016; Mohler *et al.,* 2011), composite materials (Olinda, 2010), to name but a few.

The type of process depends on the structure of the available data. For example, if the information consists of accident locations along a highway, the point process can be treated as one-dimensional, but if the information consists of the times at which accidents occurred, we have a temporal point process (TPP). If the information consists of crime locations in a city, we treat the process as spatial (SPP). However, if both the locations and the time of the crime are recorded, we then have a spatiotemporal point process (STPP).

Other possible structures for a point process can also be considered, such as the marked point process (MPP), where, in addition to the location, there is additional event-specific information, such as the height of a tree, the type of a crime, or the area of a fire. This additional information (mark) can be attached to a point that has only its spatial or temporal location, or even spatiotemporal location.

For each type of point process, there are several analysis tools (see, for example, (Baddeley *et al.,* 2015; Diggle, 2013; Illian *et al.,* 2008; Olinda, 2010; Scalon, 2025)). In this article, we will consider the case of STPP, based on the approach proposed by Stoyan *et al.* (2017), which employs the mark variogram (a method traditionally applied to marked point processes) to analyze STPP data related to fire hotspots that occurred in the Brazilian Amazon rainforest.

Forest fires in the Amazon rainforest have become an increasingly important environmental issue due to their impacts on biodiversity, carbon emissions, climate regulation, and land-use dynamics (Aragó *et al.,* 2016; Nepstad *et al.,* 2006). In many cases, fire occurrence is not randomly distributed in either space or time. Instead, fire hotspots tend to concentrate in specific regions and periods of the year, especially during the dry season, reflecting the influence of climatic conditions and vegetation characteristics favorable to fire occurrence (Corrêa, 2007). Understanding these patterns is essential for identifying critical areas and periods with higher fire risk and for supporting monitoring and prevention policies.

From a statistical perspective, fire hotspot data naturally exhibit a spatiotemporal structure, since each occurrence is associated simultaneously with a geographic location and a detection time. This means that the occurrence of a hotspot may depend not only on nearby events in space but also on previous occurrences in time. For example, neighboring areas may experience fires during similar periods due to shared environmental conditions. Likewise, persistent fire activity over time may indicate seasonal fire recurrence associated with drought periods and biomass availability (Barbosa, 2001). Therefore, investigating the existence of spatial, temporal, and spatiotemporal dependence is fundamental for understanding wildfire dynamics.

The Brazilian Amazon rainforest represents a particularly relevant study area for this type of analysis because it combines extensive forest cover, strong seasonal climatic variation, and increasing anthropogenic pressure associated with deforestation and land-use change (Aragó *et al.,* 2016; Nepstad *et al.,* 2006). These characteristics make the Amazon an important scenario for studying spatiotemporal point patterns and evaluating whether observed hotspot clusters are associated with genuine dependence structures or simply reflect variations in the intensity of the process over space and time. In this context, distinguishing between clustering caused by dependence between events and clustering induced by non-homogeneous intensity patterns becomes an important statistical challenge.

The mark variogram is a tool that describes the correlation structure between marks of a point process, quantifying how this correlation behaves as a function of the distance between points (Cressie, 1993; Illian *et al.,* 2008; Stoyan & Wälder, 2000). Its use provides important information, including: verification of the existence of spatial correlation, the rate at which the correlation between marks decreases (or increases) with increasing distance, the range of this correlation, and whether nearby points tend to have marks with similar (or dissimilar) values.

The proposal by Stoyan *et al.* (2017) consists of decomposing the STPP into two marked point processes, where one considers times as marks of spatial locations and the other considers locations as marks of times. Based on this formulation, the authors fitted a Gaussian model to the mark variogram to obtain values of the parameters of interest, such as the range and sill. The range refers to the distance within which samples are correlated, indicating that points beyond this distance are spatially (or temporally) independent. The sill is the variogram value corresponding to the range and indicates when the variability of the phenomenon stabilizes. The sill is commonly interpreted as a measure of the total variance of the data.

Stoyan *et al.* (2017) suggest visually comparing the sill of the observed spatiotemporal configuration with the sill expected under the null hypothesis (sill of a homogeneous Poisson process - HPP), which represents a configuration where locations are independent of times. For cases where the sill deviates from the expected value under the HPP hypothesis, the authors argue that this behavior is due to the fact that the observed configurations deviate from a pattern generated by a homogeneous Poisson process. However, Stoyan *et al.* (2017) do not present a formal method to test this null hypothesis. In this work, we propose to complement the approach by Stoyan *et al.* (2017) through testing the null hypothesis via the construction of empirical envelopes obtained from Monte Carlo simulations. This approach allows assessing whether the observed values of the mark variogram are compatible with those expected under different null models, including not only the homogeneous Poisson process (HPP) but also the non-homogeneous Poisson process (NHPP). Thus, we aim to provide a statistical method to test the adequacy of these models to the spatiotemporal structure present in the data.

In this work, these methods are applied to fire hotspot data, detected by satellite, in the municipality of Itapuã do Oeste, state of Rondônia (Brazilian Amazon) between 2018 and 2019. It is expected that these methods can contribute to the analysis of spatiotemporal patterns in critical ecosystems, where the detection of fire clusters in time and space can support prevention policies for this important biome.

2. Material and methods

2.1 Data

The data analyzed in this study correspond to fire hotspots observed during 2018 and 2019 in the municipality of Itapuã do Oeste, located in the state of Rondônia (RO). The municipality's biome is the Brazilian Amazon Rainforest, and of its 4081 km^2 area, approximately 2119.32 km^2 are covered by the Jamari National Forest (Legal Creation Decree: Decree n° 90.224 of September 25, 1984), as can be observed in Figure 1.

The data were obtained from the National Institute for Space Research - INPE, through the website of the Fire Monitoring Program: https://terrabrasilis.dpi.inpe.br/queimadas/bdqueimadas (INPE, 2024), considering records made by remote sensing from the reference satellite AQUA.

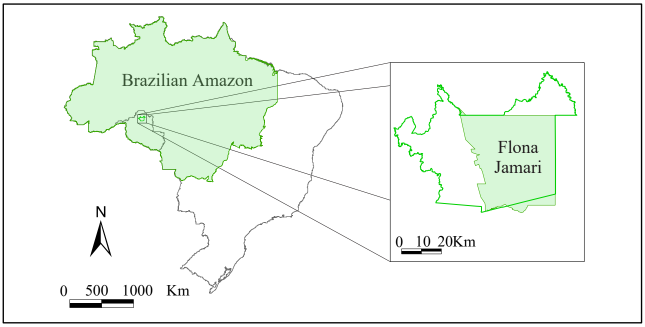

Source: Adapted from Brasil. Ministério da Agricultura, Pecuária e Abastecimento. Serviço Florestal Brasileiro (2025)

Figure 1. Location of the municipality of Itapuã do Oeste - RO and the Jamari National Forest.

The data correspond to 216 fire hotspots, that is, hotspots with temperatures above 47°C, with 111 hotspots observed in 2018 and 95 in 2019. The information used for each hotspot includes geographic coordinates and the time of occurrence, consisting of the date and hour.

For the analysis, it was necessary to convert geographic coordinates to the UTM (Universal Transverse Mercator) Cartesian coordinate system. The information about the date and time of hotspot detection was transformed into days, with the date converted to the day of the year and the hour calculated as a fraction of the day.

2.2 Point processes: definitions and properties

A point process can be understood, according to Scalon (2025), as a mathematical model for a physical phenomenon, characterized by points whose locations are realizations of a stochastic process and are randomly distributed in a continuous region, such as a time interval or uni- or multi-dimensional space. If X denotes this continuous region, a realization of the point process in X is simply a set of points in X and can be called a *point pattern*.

2.2.1 Spatiotemporal point processes

A spatiotemporal point process (STPP) is a stochastic process that generates a countable set of points $\{(\mathbf{s}_i, t_i) : i = 1, \ldots, n\}$, where $\mathbf{s}_i \in S \subset \mathbb{R}^2$ and $t_i \in T \subset \mathbb{R}^+$, so that its study is considered in the Cartesian product $\mathbb{R}^2 \times \mathbb{R}^+$ (Diggle, 2013).

In the analysis of an STPP, its first- and second-order properties are generally considered. According to Gabriel *et al.* (2013) and Snyder & Miller (1991), the first-order properties of a spatiotemporal point process can be described by its spatiotemporal intensity function, given by

$$\lambda(\mathbf{s}, t) = \lim_{|d\mathbf{s}|,|dt| \to 0} \left\{ \frac{E[N(d\mathbf{s}, dt)]}{|d\mathbf{s}||dt|} \right\}, \tag{1}$$

where $d\mathbf{s}$ defines a small region around the location $\mathbf{s}$, $|d\mathbf{s}|$ is its area, dt is a small interval containing time t, $|dt|$ is the length of this interval, and $N(d\mathbf{s}, dt)$ is the number of events in $d\mathbf{s} \times dt$. A process where $\lambda(\mathbf{s}, t) = \lambda$ for all $(\mathbf{s}, t)$ is said to be homogeneous. Informally, $\lambda(\mathbf{s}, t)$ can be understood as the average number of events per unit volume around the location $(\mathbf{s}, t)$.

Regarding the second-order properties of a spatiotemporal point process, Gabriel *et al.* (2013) and Snyder & Miller (1991) point out that they describe the relationship between numbers of events in pairs of subregions within $S \times T$ and are given in terms of the intensity function

$$\lambda_2\Big((\mathbf{s}_i, t_i), (\mathbf{s}_j, t_j)\Big) = \lim_{|d\mathbf{s}_i \times dt_i|, |d\mathbf{s}_j \times dt_j| \to 0} \left\{ \frac{E[N(d\mathbf{s}_i \times dt_i)N(d\mathbf{s}_j \times dt_j)]}{|d\mathbf{s}_i \times dt_i||d\mathbf{s}_j \times dt_j|} \right\}, \tag{2}$$

where $d\mathbf{s}_i \times dt_i$ and $d\mathbf{s}_j \times dt_j$ are small cylinders containing the points $(\mathbf{s}_i, t_i)$ and $(\mathbf{s}_j, t_j)$, respectively.

Considering the study of these properties, the goal is then to compare the events of the observed point pattern with a null model given by complete spatiotemporal randomness (CSTR), which is the case of the homogeneous Poisson process in space-time. CSTR occurs, according to Gabriel *et al.* (2013), when

- For some $\lambda > 0$, the number $N(S \times T)$ of events within the region $S \times T$ follows a Poisson distribution with mean $\lambda|S||T|$, where $|.|$ denotes the area (two-dimensional) or length (one-dimensional), depending on the context.
- Given $N(S \times T) = n$, the n events in $S \times T$ form an independent random sample from the uniform distribution on $S \times T$.

According to Gabriel *et al.* (2013), for the case of the homogeneous Poisson process, the first- and second-order intensities reduce to constants $\lambda(\mathbf{s}, t) = \lambda$ and $\lambda_2\Big((\mathbf{s}_i, t_i), (\mathbf{s}_j, t_j)\Big) = \lambda^2$. Values greater or smaller than these parameters would therefore indicate, informally, how much more or less likely it is that a pair of events will occur at specific locations of a Poisson process with the same intensity.

The assumptions of stationarity and isotropy about a point process are made to facilitate the analyses. According to Lloyd (2010) and Scalon (2025), the term stationarity is used to refer to the result of some process that has similar properties at all locations in the region of interest, more specifically, the process is said to be stationary if its statistical properties are invariant under translation. According to Scalon (2025), the process is said to be isotropic if its statistical properties are invariant under rotation. The property of isotropy does not make sense for temporal point processes. A spatiotemporal point process is second-order stationary, according to Gabriel *et al.* (2013), if:

- in space, if $\lambda(\mathbf{s}, t) \equiv \lambda(t)$ and $\lambda_2\Big((\mathbf{s}_i, t_i), (\mathbf{s}_j, t_j)\Big) = \lambda_2(\mathbf{s}_i - \mathbf{s}_j, t)$, i.e., it is invariant under translation in space (homogeneous first-order intensity and second-order intensity depends only on the relative distance), but varies in time;
- in time, if $\lambda(\mathbf{s}, t) \equiv \lambda(s)$ and $\lambda_2\Big((\mathbf{s}_i, t_i), (\mathbf{s}_j, t_j)\Big) = \lambda_2(\mathbf{s}, t_i - t_j)$, i.e., the first-order intensity is constant in time but varies in space, and the second-order intensity varies in space but depends only on the relative temporal distance between events;
- in space and time, if $\lambda(\mathbf{s}, t) \equiv \lambda$ and $\lambda_2\Big((\mathbf{s}_i, t_i), (\mathbf{s}_j, t_j)\Big) = \lambda_2(\mathbf{s}_i - \mathbf{s}_j, t_i - t_j)$, that is, it is invariant under translation in time and space.

The process will also be isotropic if $\lambda_2((\mathbf{s}_i, t_i), (\mathbf{s}_j, t_j)) = \lambda_2(r, t)$, where (r, t) is the spatiotemporal distance vector, $r = ||\mathbf{s}_i - \mathbf{s}_j||$ and $t = |t_i - t_j|$, that is, it is invariant under rotation.

For the case where the process is non-stationary, that is, we have a non-homogeneous first-order intensity, the point pattern can be compared to a NHPP which, despite having a varying intensity, does not exhibit a spatiotemporal correlation structure between events. This process can be obtained by replacing the constant intensity λ of the homogeneous Poisson process with an intensity function $\lambda(\mathbf{s}, t)$ that varies in space, time, or both (Gabriel *et al.,* 2013).

According to these authors, a NHPP can be defined based on the following postulates:

- The number $N(S \times T)$ of events within the region $S \times T$ follows a Poisson distribution with mean $\int_S \int_T \lambda(\mathbf{s}, t) dt ds$.
- Given $N(S \times T) = n$, the n events in $S \times T$ form an independent random sample from the distribution on $S \times T$ with a probability density function proportional to $\lambda(\mathbf{s}, t)$.

Gabriel *et al.* (2013) state that for a Poisson process with intensity $\lambda(\mathbf{s}, t)$, the second-order intensity is $\lambda_2\big((\mathbf{s}_i, t_i), (\mathbf{s}_j, t_j)\big) = \lambda(\mathbf{s}_i, t_i)\lambda(\mathbf{s}_j, t_j)$.

These concepts enable the structuring of summary statistics such as the K function (Diggle *et al.*, 1995; Diggle & Gabriel, 2010; Gabriel & Diggle, 2009; Scalon, 2025), which is theoretically known for the cases of an HPP or NHPP. The K function obtained for the observed configuration is then compared with the theoretical K function, and based on this comparison, the researcher can proceed with more specific analyses.

2.2.2 Simulation envelopes

Just as for a random sample it is necessary to perform some hypothesis test to verify whether the data follow a certain distribution or not, for the case of an SPP, an equivalent approach is recommended.

According to Wiegand & Moloney (2013), approaches using summary statistics such as the K function require the comparison of observed patterns and patterns created by a null model to assess their correspondence. Scalon (2025) points out that the most practical alternative is to use Monte Carlo simulations to produce realizations of the stochastic point process underlying the specific null model to indicate the range of statistical variation under the null model.

In this procedure, each simulation of the null model generates a point pattern, and the test statistic is calculated for each simulated pattern.

Wiegand & Moloney (2013) point out that since the null model is stochastic, the results of the test statistics in each of the different simulated patterns do not present an exact correspondence with each other but instead exhibit fluctuations around the theoretically expected value. Thus, the goal of the approach using the simulation envelope is to determine whether the test statistic of the observed data is outside the range of stochastic fluctuations produced by the null model.

For this procedure, let us consider, according to Baddeley *et al.* (2015), any summary function S for point processes. To perform the test, first the function S is calculated for the observed data, $S_{obs}(r)$. Then, m synthetic point processes are generated, simulated from the null hypothesis, and their respective estimated S functions are obtained for each simulation, $S^{(1)}(r),\ S^{(2)}(r), \ldots,\ S^{(m)}(r)$.

To apply the Monte Carlo test principle, Baddeley *et al.* (2015) point out that it is necessary to reduce the function $S(r)$ to a simple number T, which will serve as the test statistic. One approach presented by the authors consists of specifying a distance $r = r_0$ and defining $T = S(r_0)$, which is the value of the summary function at that specific distance. According to the authors, under the null hypothesis, the values of $\widehat{S}(r_0)$ for the data and for the simulated patterns are statistically equivalent random variables, and the Monte Carlo test principle applies. Thus, the two-sided Monte Carlo test with significance level $\alpha = 2/(m+1)$ rejects the null hypothesis if the value $t_{obs} = S_{obs}(r_0)$ is outside the range of all values obtained by simulation $t_1 = S^{(1)}(r_0),\ t_2 = S^{(2)}(r_0), \ldots,\ t_m = S^{(m)}(r_0)$, that is, if $t_{obs} > \max_j t_j$ or $t_{obs} < \min_j t_j$. This rule is, according to Scalon (2025), equivalent to constructing the plot of the upper and lower envelopes given by

$$\begin{aligned} U(r) &= \max_j S^{(j)}(r)\left\{S^{(1)}(r),\ S^{(2)}(r), \ldots,\ S^{(m)}(r)\right\} \\ L(r) &= \min_j S^{(j)}(r)\left\{S^{(1)}(r),\ S^{(2)}(r), \ldots,\ S^{(m)}(r)\right\}, \end{aligned} \tag{3}$$

cutting it with a vertical line that intersects the horizontal axis at $r = r_0$, and the null hypothesis is rejected if the value of the observed function $S_{obs}(r)$ is outside the interval bounded by these envelopes at that pre-specified distance $r = r_0$.

According to Wiegand & Moloney (2013), to obtain a 5% significance level, one possibility is to use the observed data pattern plus 199 simulations under the null model to construct the envelope.

Consider, for example, that an observed pattern actually follows an HPP. In this case, the risk that $\hat{S}(r)$ estimated for this observed pattern is outside the envelope limits is 5/200 being below and 5/200 for being above. More generally, the simulation envelopes can be defined as the s-th highest and lowest values of the test statistic, taken from m simulations of the null model with significance level $\alpha = 2\frac{s}{m+1}$ for the two-tailed test.

2.2.3 Marked point processes

A point process is said to be mark when, in addition to the spatial location of events, there is additional information (mark) attached to each event. According to Chiu *et al.* (2013), a marked point process in $\mathbb{R}^d$ is a random sequence $X_m = \{(\mathbf{s}_i, m_i)\}$, where the points $\mathbf{s}_i$ together constitute the unmarked point process in $\mathbb{R}^d$, and the values m_i are the marks corresponding to each point $\mathbf{s}_i$, that is, $m_i = m(\mathbf{s}_i)$. Considering here $d = 2$ and that the marks belong to the mark space $\mathcal{M}$, the study of marked point processes is given in $\mathbb{R}^2 \times \mathcal{M}$. Daley & Vere-Jones (2002) refer to the unmarked point process X as the *base process*, which will also be considered here.

Regarding the nature of the marks, they can be continuous or discrete/categorical variables. An example of a continuous variable is the diameter at breast height of trees in a forest stand, and in the discrete case, the species of the trees.

It is important to highlight that marked point pattern data has similarities with geostatistical data, which also consist of information about locations $\mathbf{s}$ and associated values $Z(\mathbf{s})$. However, as Scalon (2025) states, the goal of geostatistics is to estimate spatially continuous phenomena based on measurements made at points chosen for this purpose. In the case of marked point patterns, the points do not represent the locations chosen for measurement purposes but the exact locations where the analyzed objects occurred. Thus, according to Illian *et al.* (2008), the analysis of geostatistical data and marked point process data have completely different objectives and apply different methods, so the misuse of geostatistical methods in marked point processes can produce incorrect results. Since marks only exist at the event locations and not throughout the study region, a variable that occurs throughout the region and is intended to be incorporated into the point pattern analysis should then be treated as a covariate and not as a mark.

Considering that marks can be of discrete or continuous nature, there are specific methods to analyze each of these cases. Our analysis here focuses on the continuous case, where $\mathcal{M} = \mathbb{R}$. Methods for analyzing categorical marks can be found in Baddeley *et al.* (2015) and Illian *et al.* (2008), while methods for continuous marks can be found in Olinda (2010).

For the case of a marked point process, the assumption of stationarity is also considered. Consider, according to Illian *et al.* (2008), the marked point process X_m given by $X_m = \{(\mathbf{s}_1, m_1), (\mathbf{s}_2, m_2), \ldots\}$ and $X_m^s = \{(\mathbf{s}_1 + \mathbf{s}, m_1), (\mathbf{s}_2 + \mathbf{s}, m_2), \ldots\}$ the process translated by $\mathbf{s}$. Note that in X_m^s the marks remain the same, but the points are translated. From this, we have that a marked point process X_m is stationary if and only if

$$X_m \stackrel{d}{=} X_m^s,$$

that is, the marked point process X_m and the spatial marked point process translated by $\mathbf{s}$ have the same distribution. If the process, in addition to having this invariance under translation, is also invariant under rotation, it is said to be isotropic.

As in the cases presented earlier, a marked point process can be studied by its first- and second-order properties, given in terms of intensity functions. In general, Zhang & Zhuang (2014) express the k-th order intensity function by

$$\lambda_k\Big((\mathbf{s}_1, m_1), \ldots, (\mathbf{s}_k, m_k)\Big) = \lim_{|d\mathbf{s}_i \times dm_i| \to 0,\ i=1,\ldots,k} \left\{ \frac{E[N(d\mathbf{s}_1 \times dm_1) \ldots N(d\mathbf{s}_k \times dm_k)]}{|d\mathbf{s}_1 \times dm_1| \ldots |d\mathbf{s}_k \times dm_k|} \right\} \tag{4}$$

where $(\mathbf{s}_i, m_i)$ are distinct pairs of points and marks in $\mathbb{R}^2 \times \mathbb{R}$, $d\mathbf{s}_i \times dm_i$ is an infinitesimal region containing $(\mathbf{s}_i, m_i)$, and $|d\mathbf{s}_i \times dm_i|$ is the measure of $d\mathbf{s}_i \times dm_i$.

From λ_k, as in the case of STPP, functions are defined that are used to describe the data of a spatial marked point process, which will not be considered here; the interested reader can find them, for example, in Baddeley *et al.* (2015).

In the case of spatial marked point processes with quantitative marks, the interest lies, as pointed out by Wiegand & Moloney (2013), in characterizing the process that distributed the marks over the events, while the characteristics of the unmark pattern itself (how the events are distributed, whether the intensity is constant or not, or whether there is any spatial correlation structure between them) are generally not of interest.

In a marked point process, the goal is to describe the variability in the distribution of the marks, as well as the existing correlations between the marks and the points. An assumption made in many cases is to assume that marks are independent and identically distributed (i.i.d.). However, the mark m_i may depend on its location $\mathbf{s}_i$.

In marked point processes, an alternative form of randomness is known as *random labeling*. While complete randomness describes events that occur randomly in a study area, random labeling simply describes the points of a process being randomly marked, independent of the base process distribution.

In the case of random labeling, the marks of the process are, according to Pawlas (2009), independent and identically distributed (i.i.d.) and, moreover, are independent of the points.

To test a dataset under the random labeling hypothesis, the procedure makes use of simulation envelopes, where in this case, the m "simulations" are obtained by keeping the locations of the base process fixed and permuting the marks m times, where the marks are randomly assigned to each location. For each permutation, the test statistic of interest is computed, the envelopes are constructed at the end, and compared with the result of the original data, in the same way as shown earlier. Rejecting the random labeling hypothesis means that the marks are not independent and identically distributed and were not randomly assigned to their locations, indicating that there is a correlation structure between them and with the points.

2.2.4 The mark variogram

The mark variogram (Baddeley *et al.,* 2015; Cressie, 1993; Illian *et al.,* 2008; Stoyan & Wälder, 2000; Wälder & Stoyan, 1996) for a stationary marked point process is defined by

$$\gamma(r) = \frac{1}{2}\mathbb{E}\left[\left(m_i - m_j\right)^2 \middle| \, |\mathbf{s}_i - \mathbf{s}_j| = r\right]. \tag{5}$$

Thus, $2\gamma(r)$ is the expected quadratic difference between the values of two marks whose corresponding points are separated by a distance r. According to Stoyan *et al.* (2017), the behavior of $\gamma(r)$ as a function of r provides valuable information about the spatial correlations between the marks of the process. Three aspects of this information highlighted by the authors are described below.

1. If the marks of nearby points are similar for small values of r, $\gamma(r)$ has small values. This is a natural behavior in many cases, but Stoyan *et al.* (2017) point out, however, that this is not the only possibility and report the example presented in Baddeley *et al.* (2015) regarding the *spruces* dataset (a typical tree of temperate regions), where there is an increase in variation at very short distances. A possible interpretation, according to the authors, is that for very large trees found close to each other, there must be at least one that is small.

2. As r increases, $\gamma(r)$ often increases and shows asymptotic convergence toward a constant value, that is (Illian *et al.,* 2008):
$$\lim_{r\to\infty} \gamma(r) = \sigma^2_\mu. \tag{6}$$

This constant value is called the *sill* or *variance of the marks*. It may happen, however, that $\gamma(r)$ decreases in some intervals of r, as in the case mentioned earlier. According to Stoyan *et al.* (2017), the speed of convergence is related to the speed of decline of the spatial correlation of the marks with increasing inter-point distances. And the value of r at which the sill is reached is called the *range*. If it exists, the range is a valuable correlation parameter.

3. The behavior of $\gamma(r)$ near the origin, denoted by $\gamma(0+)$, is also often of interest. $\gamma(0+)$ is called the *nugget effect* and may happen, according to the authors, to be positive and not disappear, as might be expected. $\gamma(0+)$ reflects the spatial aggregation of nearby points with different marks. That is, a positive value of $\gamma(0+)$ indicates that nearby points tend to have significantly different marks. And in the case of $\gamma(0+)$ being positive and constant for $r > 0$, it is then referred to as a *pure nugget effect*.

2.3 Analysis of STPP using the mark variogram

Considering the spatiotemporal point process $X = \{(\mathbf{s}_1, t_1), (\mathbf{s}_2, t_2), \ldots\}$ and assuming that there are no coincident points and the process occurs in a time window $T = [0, \tau]$ and space window W, given by a rectangle with sides a and b, Stoyan *et al.* (2017) state that a spatiotemporal point process can be transformed into a marked point process in two ways.

The first is to reinterpret the process X as a mark process X_T by taking the times t_i as marks of the locations $\mathbf{s}_i$, that is, $X_T = \{(\mathbf{s}_i, t(\mathbf{s}_i))\}$. The second way is to reinterpret the process X as a mark process X_W by taking the locations $\mathbf{s}_i$ as marks of the times t_i, that is, $X_W = \{(t_i, \mathbf{s}_i(t_i))\}$.

Stoyan *et al.* (2017) state that the invariance properties of the process X are transmitted to X_T and X_W.

Let X be a stationary process where $\mathbf{s}_i \in \mathbb{R}^2$ and $t \in \mathbb{R}$ and

$$X \overset{d}{=} X^{s,t} \tag{7}$$

where $X^{s,t}$ is the translated process $X^{s,t} = \{(\mathbf{s}_1 + \mathbf{s}, t_1 + t), (\mathbf{s}_2 + \mathbf{s}, t_2 + t), \ldots\}$. Stoyan *et al.* (2017) point out that if X is completely stationary, then X_T and X_W are stationary as marked point processes.

2.3.1 The mark variograms $\gamma_{sp}(r)$ and $\gamma_{te}(t)$

For each of the processes X_T and X_W, Stoyan *et al.* (2017) consider the respective mark variograms. According to the authors, both describe the extent of correlations between the spatial and temporal components, in particular the extent of spatiotemporal clustering.

For the case of the process X_T, Stoyan *et al.* (2017) define the spatial mark variogram $\gamma_{sp}(r)$ by

$$\gamma_{sp}(r) = \frac{1}{2}\mathbb{E}\left[(t(\mathbf{u}) - t(\mathbf{v}))^2 \middle| \, \mathbf{u}, \mathbf{v} \in X_{space}\right] \tag{8}$$

where $t(\mathbf{s})$ is the time mark of the point at location $\mathbf{s}$, and X_{space} is the spatial component of the spatiotemporal point process. This function has basically the same structure as that presented in equation (5) with the only difference that the marks are given by times.

The temporal mark variogram $\gamma_{te}(t)$ is given by

$$\gamma_{te}(t) = \frac{1}{2}\mathbb{E}\left[(\mathbf{s}(l) - \mathbf{s}(k))^2 \middle| \, l, k \in X_{time}\right] \tag{9}$$

where $\mathbf{s}(t)$ is the spatial mark of the point at time t, and X_{time} is the temporal component of the spatiotemporal point process. In this case, the locations are points in $\mathbb{R}$ and the marks are in $\mathbb{R}^d$. It is also noted that instead of the spatial distance r, what is considered is the temporal distance t, and instead of the quadratic difference of the marks, their quadratic distance is considered.

Regarding the spatiotemporal behavior of the process X, Stoyan *et al.* (2017) point out that $\gamma_{sp}(r)$ provides valuable information and presents the following characteristics:

1. If points clustered in space also tend to be clustered in time, then $\gamma_{sp}(r)$ has small values for small r.
2. As r increases, $\gamma_{sp}(r)$ often increases and shows asymptotic behavior, converging toward a sill value. The speed of this convergence is related to the speed of increase in the variability of the appearance times of the members of point pairs with increasing distance r between the points. This means that if the convergence toward the sill is fast, the extent of spatiotemporal dependence is present for short distances. And if this convergence is slow, the extent of spatiotemporal dependence exists for larger distances.
3. The behavior of $\gamma_{sp}(r)$ near the origin can be characterized by a nugget effect. According to the authors, it may happen that, in the same region of space, clusters of points appear at different times.

The properties of $\gamma_{te}(t)$, in relation to the spatiotemporal point process X and presented by Stoyan *et al.* (2017), are analogous to the case of $\gamma_{sp}(r)$.

2.3.2 Estimation of $\gamma_{sp}(r)$ and $\gamma_{te}(t)$

Assuming that the point process is stationary, an estimator for $\gamma_{sp}(r)$ presented by Stoyan *et al.* (2017) is:

$$\widehat{\gamma}_{sp}(r) = \frac{\sum^{\neq}_{\mathbf{s}_1,\mathbf{s}_2 \in W} \frac{\frac{1}{2}(|t_1-t_2|)^2 \kappa_\epsilon(|\mathbf{s}_1-\mathbf{s}_2|-r)}{2\pi r e_2(\mathbf{s}_1,\mathbf{s}_2)}}{\sum^{\neq}_{\mathbf{s}_1,\mathbf{s}_2 \in W} \frac{\kappa_\epsilon(|\mathbf{s}_1-\mathbf{s}_2|-r)}{2\pi r e_2(\mathbf{s}_1,\mathbf{s}_2)}}, \quad 0 < \epsilon < r, \tag{10}$$

where κ_ϵ is a one-dimensional kernel function with bandwidth ϵ, and $e_2(\mathbf{s}_1, \mathbf{s}_2))$ is a generic edge-correction factor. According to Wälder & Wälder (2008), kernel-based estimators are useful for obtaining smoother functions when exact distances r between point pairs are rare.

The bandwidth parameter ϵ determines the degree of smoothing of the kernel estimator and directly affects the empirical behavior of the variogram. Bandwidth selection can be performed using the automatic procedures available in the *stpp* package in R, based on kernel smoothing methods described by Diggle (1985) and Berman & Diggle (1989). The bandwidth is selected by minimizing an approximation to the mean squared error criterion, providing a balance between estimator variability and oversmoothing.

Stoyan *et al.* (2017) propose a simplified estimator without edge correction:

$$\widehat{\gamma}_{sp}(r) = \frac{\sum^{\neq}_{\mathbf{s}_1,\mathbf{s}_2 \in W} \frac{1}{2}(|t_1 - t_2|)^2 \kappa_\epsilon(|\mathbf{s}_1 - \mathbf{s}_2| - r)}{\sum^{\neq}_{\mathbf{s}_1,\mathbf{s}_2 \in W} \kappa_\epsilon(|\mathbf{s}_1 - \mathbf{s}_2| - r)}. \tag{11}$$

The temporal variogram estimator is analogous:

$$\widehat{\gamma}_{te}(t) = \frac{\sum^{\neq}_{t_1,t_2 \in T} \frac{1}{2}(|\mathbf{s}_1 - \mathbf{s}_2|)^2 \kappa_\delta(|t_1 - t_2| - t)}{\sum^{\neq}_{t_1,t_2 \in T} \kappa_\delta(|t_1 - t_2| - t)}, \tag{12}$$

where δ is the temporal bandwidth parameter.

2.3.3 The Gaussian Model

The Gaussian model is defined according to Montero *et al.* (2015), as

$$\gamma(|h|) = m\left(1 - \exp\left(\frac{-|h|^2}{a^2}\right)\right) \tag{13}$$

where $|h|$ is the distance between two locations; a is the correlation range, that is, the distance within which samples are correlated; m is the sill, which is the value of the variogram corresponding to the range a.

The value of $\gamma(0)$ is the nugget effect and is theoretically equal to zero. However, in practice, as noted by Camargo *et al.* (2004), when $h \to 0$, $\gamma(|h|)$ approaches a positive value C_0. This value is related to the discontinuity of the variogram for distances smaller than the minimum distance between samples. Thus, the nugget effect represents the component of spatial variability that may be due to measurement errors or small-scale variability that cannot be observed by sampling. Therefore, the sill value is given by $m = C_0 + C_1$, where C_1 is referred to as the "contribution."

When using the Gaussian model, the objective of Stoyan *et al.* (2017) was not to make predictions from the fitted model, nor to select among multiple variogram candidates. The authors' goal was simply to use the Gaussian model as a tool to obtain estimates of the range and sill parameters in order to describe the correlation structure in the point process. Following this rationale, we adopt the same model as an established structural benchmark for the mark variogram method.

2.3.4 Considerations on the Variograms $\gamma_{sp}(r)$ and $\gamma_{te}(t)$

A result presented by Stoyan *et al.* (2017) for the variograms $\gamma_{sp}(r)$ and $\gamma_{te}(t)$ is their theoretical value under the assumption of complete spatio-temporal randomness, i.e., a homogeneous Poisson process. Considering a spatial window W given by a rectangle with sides a and b, and a temporal window $T = [0, \tau]$, we have

$$\gamma_{sp}(r) = \begin{cases} 0 & \text{for} \quad r = 0 \\ c_{sp} & \text{for} \quad r > 0 \end{cases} \qquad \text{and} \qquad \gamma_{te}(t) = \begin{cases} 0 & \text{for} \quad t = 0 \\ c_{te} & \text{for} \quad t > 0 \end{cases} \tag{14}$$

where $c_{sp} = \dfrac{\tau^2}{12}$ and $c_{te} = \dfrac{a^2 + b^2}{12}$.

After performing estimation and fitting the Gaussian model to simulated data from a STPP with different structures and to real data, the authors Stoyan *et al.* (2017) concluded that the estimated and fitted variograms yielded results consistent with the data structure. Another aspect highlighted by the authors is that, using the proposed estimator, edge effects and lack of homogeneity can be ignored. Furthermore, the shape of the window is also irrelevant, making the estimator robust for different types of spatial and temporal windows.

The sill value obtained from fitting the Gaussian model to $\gamma_{sp}(r)$ and $\gamma_{te}(t)$ was compared with the values of c_{sp} and c_{te}, respectively. For cases where the sill value deviated from the expected value for a HPP, the authors argued that this was due to the fact that the data from the analyzed patterns were far from exhibiting an HPP structure. However, they did not provide a way to verify this using the variograms.

In this work, for the analyzed data, this verification was performed using a Monte Carlo simulation approach to construct the envelope under the null models of an HPP and a NHPP.

2.3.5 Data Analysis

In the analysis of the data based on the proposal by Stoyan *et al.* (2017), for each of the variograms $\gamma_{sp}(r)$ and $\gamma_{te}(t)$, estimation and fitting of the Gaussian model were performed.

Subsequently, to investigate the deviations of the estimated variogram from the expected behavior under complete randomness, envelopes were constructed from 199 simulations of an HPP, with the same number of points and in the same spatio-temporal region as the data.

Another null model considered in these analyses was the NHPP. This is due to the fact that if the variogram exhibits a sill much lower than expected for an HPP, then very small variability between locations and times may form clusters that are not due to a second-order effect. That is, the process may be non-stationary, possessing a non-homogeneous first-order intensity, such that there is a trend effect in the occurrences of heat foci rather than dependence.

In the case of simulating an NHPP, the non-homogeneous intensity $\lambda(\mathbf{s}, t)$ can be introduced as a function of the coordinates or as a three-dimensional *array* object (which was the case used here). The construction of this *array* object can be done by estimating the intensity of the observed process using kernel functions. A detailed description of this process is provided in Gabriel *et al.* (2013).

If the estimated variogram does not remain within the envelope, even when considering the NHPP as the null model, then the observed clustering behavior is not simply due to a trend effect but rather to dependence.

2.4 Softwares

All analyses were performed using functions developed in the computational environment of the R software (R Core Team, 2024). The libraries used were *spatstat* (Baddeley & Turner, 2005) for spatial data simulation and exploratory analysis; *stpp* (Gabriel *et al.,* 2024), for spatio-temporal data simulation and calculation of the variograms $\gamma_{sp}(r)$ and $\gamma_{te}(t)$; and *geoR* (Ribeiro Jr & Diggle, 2025), for fitting the Gaussian model to the variogram.

3. Results and discussion

3.1 Descriptive analysis

First, we consider the temporal distribution of fire hotspots. Figure 2 shows the number of fire hotspots in Itapuã do Oeste - RO, by month, during the study period from 2018 to 2019.

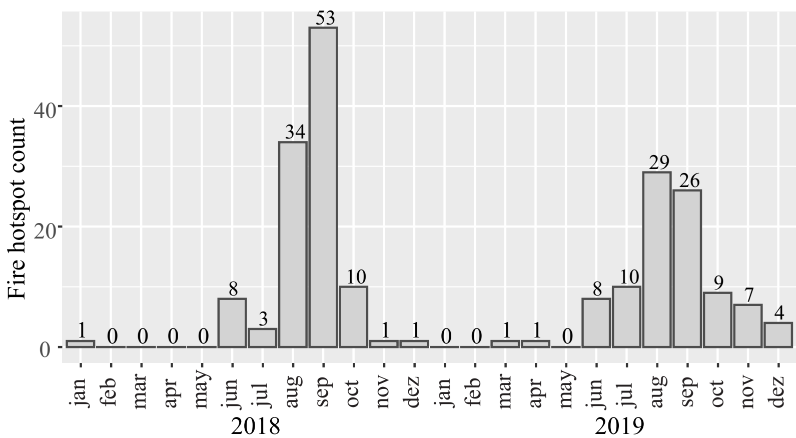

Figure 2. Monthly distribution of fire hotspots in Itapuã do Oeste - RO between 2018 and 2019.

Figure 2 shows a seasonal pattern in the number of fire hotspots, with the majority of occurrences concentrated between June and October for both 2018 and 2019. Within each year, the distribution is non-uniform, with August and September showing the highest number of occurrences. This period of high hotspot incidence coincides with the dry season, characterized by low rainfall, low air humidity, and high atmospheric temperatures. According to Corrêa (2007), these factors are favorable for fire occurrences in natural areas.

Regarding the spatial distribution of fire hotspots, Figure 3 shows the locations of each hotspot recorded between 2018 and 2019, as well as for each year separately.

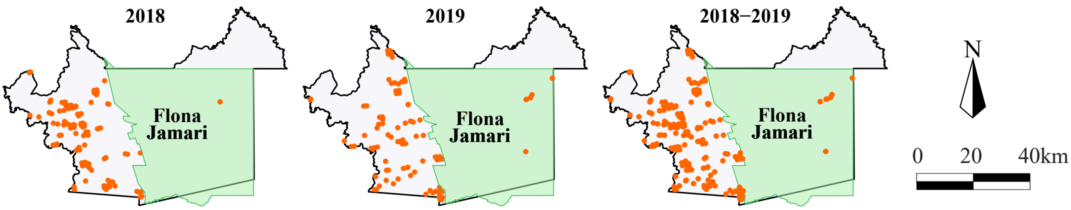

Figure 3. Spatial distribution of fire hotspots in Itapuã do Oeste - RO between 2018 and 2019.

Figure 3 shows that most hotspots are located outside the Jamari National Forest area. This is an important finding, as it reinforces the importance of environmental conservation units in fire prevention and biodiversity preservation. As noted by Ramos *et al.* (2016), conservation units' ability to control land use and human demographic pressure tends to minimize or prevent fire occurrences within their boundaries. In the Amazon, although many conservation units have limited infrastructure and lack fire brigades, they have proven effective in containing fires and deforestation (Nepstad *et al.,* 2006).

Additionally, regarding hotspot distribution, there appears to be a "migration" of hotspot locations from 2018 to 2019. A possible explanation is that areas burned in one year did not experience recurrence the following year. This finding aligns with results from Barbosa (2001), who state that most annually burned areas are those that did not burn the previous year, indicating greater biomass availability for burning in subsequent periods due to fuel accumulation.

3.2 STPP analysis using the mark variogram

The results of the unmark spatiotemporal point process analysis for fire hotspot data using the approach proposed by Stoyan *et al.* (2017), including simulation envelopes, are shown in Figure 4.

Figure 4 (a) shows the estimated mark variograms $\gamma_{sp}(r)$ and $\gamma_{te}(t)$ fitted with the Gaussian model for fire hotspots in Itapuã do Oeste - RO between 2018 and 2019, along with the respective Gaussian model parameters and the theoretical variogram values expected for an HPP. For $\gamma_{sp}(r)$, the Gaussian model's sill value corresponds to approximately 87% of that expected for an HPP. A range of approximately 4 kilometers is also observed, indicating a correlation (dependence) structure between occurrence times up to this distance, beyond which the pattern becomes random. This behavior can also be seen in Figure 4 (b), where for distances between approximately 1 and 4 kilometers, $\hat{\gamma}_{sp}(r)$ lies outside the envelope constructed under the HPP null model and remains within it thereafter. Since the nugget effect value lies below the sill, this behavior indicates that nearby points in space also occurred close in time, suggesting some form of fire hotspot clustering.

For $\gamma_{te}(t)$ in Figure 4 (a), the Gaussian model shows a range of approximately 66 days, meaning that within this time interval, the model indicates a correlation (dependence) structure between fire occurrences. However, the model's sill is approximately half of that expected for an HPP, meaning that even for large time intervals, the variability between hotspots is much smaller than expected under an HPP, indicating a temporal clustering structure. Indeed, Figure 4 (b) shows that $\hat{\gamma}_{te}(t)$ always remains outside the envelope, leading to rejection of the homogeneous Poisson process hypothesis.

For this latter case, envelopes were also constructed using 199 simulations of a non-homogeneous Poisson process where the intensity $\lambda(s, t)$ was given by an array, with each element being the spatiotemporal intensity value of the observed process. Figure 4 (c) shows that $\hat{\gamma}_{te}(t)$ remains entirely

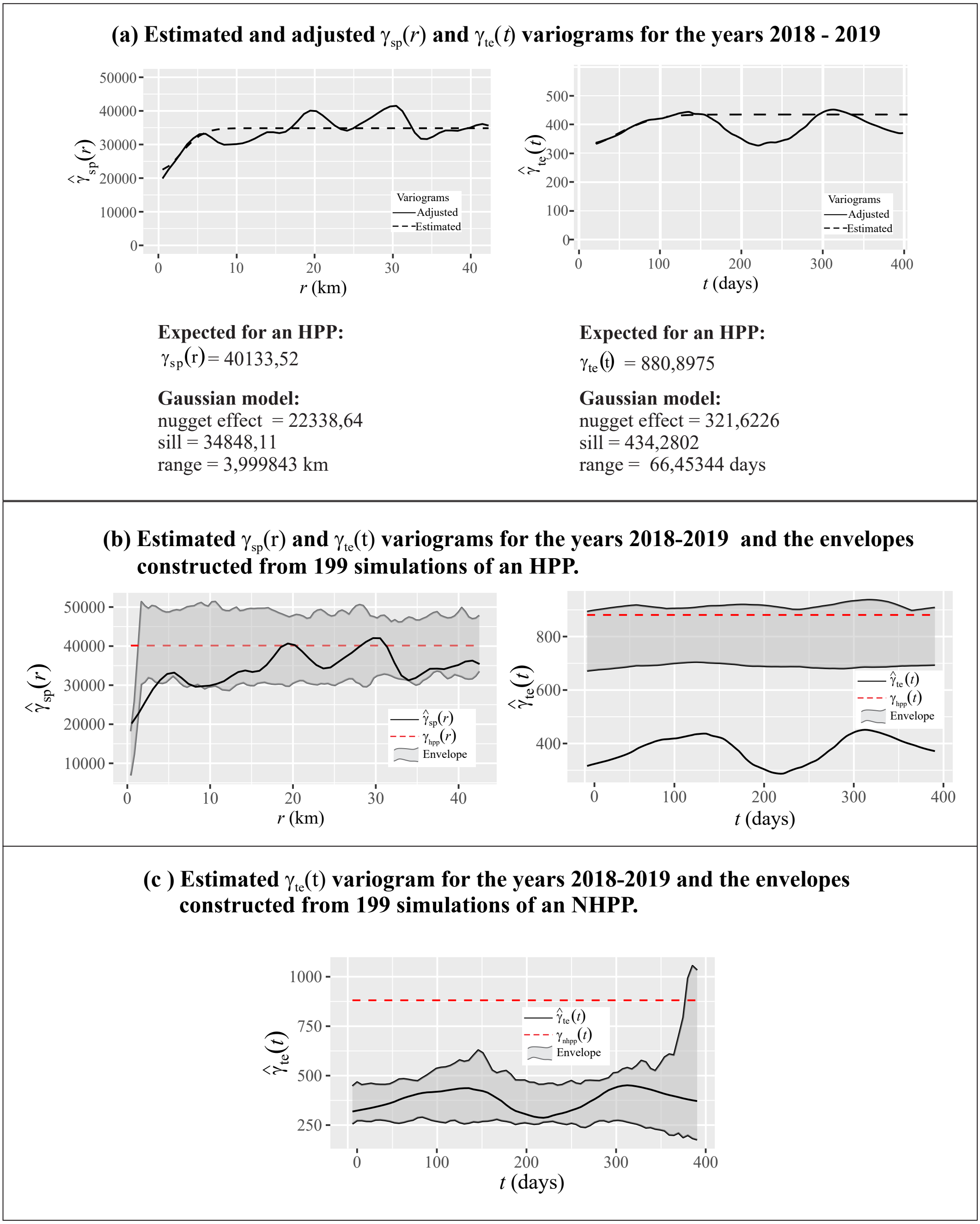

Figure 4. Results of spatiotemporal analysis for the 2018-2019 period using the Gaussian model and simulation envelopes.

within the simulation envelopes under the NHPP assumption, indicating that the observed temporal clustering pattern can be explained by first-order intensity variation rather than genuine second-order dependence between events. In contrast, under the HPP assumption, the same pattern appears to exhibit apparent structural clustering because the homogeneous model does not account for variations in the process intensity over space and time. Therefore, the comparative evaluation between HPP and NHPP envelopes shows that part of the apparent clustering behavior is induced by non-homogeneous intensity effects rather than by interaction between fire hotspots.

Overall, the spatiotemporal pattern of fire hotspots during the study period suggests stronger first-order intensity variation than genuine dependence. One possible explanation is that temporally, hotspots tend to occur during the dry season. This seasonal behavior is consistent with studies showing that fire occurrence in the Amazon is strongly associated with dry periods and climatic conditions favorable to biomass burning (Aragó *et al.,* 2016; Corrêa, 2007). Spatially, cases tend to occur in areas without environmental protection, with humans being the main agents initiating fires (ICMBio, 2016). Similarly, the spatial concentration of hotspots near non-protected areas is compatible with studies indicating that anthropogenic activities and land-use change are important drivers of fire occurrence in the Amazon region (Nepstad *et al.,* 2006).

Additionally, in spatiotemporal analyses using the variograms $\gamma_{sp}(r)$ and $\gamma_{te}(t)$, simulation envelopes play an important role in complementing the approach proposed by Stoyan *et al.* (2017). When empirical variograms deviate from the theoretical behavior expected under complete spatial randomness, the Gaussian model alone does not allow distinguishing whether the observed pattern is caused by genuine dependence between events or by first-order intensity variation. In this context, the use of NHPP-based envelopes becomes particularly important because it allows separating non-homogeneous intensity effects from true second-order interaction structures, thereby reducing misleading interpretations of clustering behavior. This distinction is particularly important because non-homogeneous intensity patterns may produce apparent clustering effects even in the absence of true interaction between events, leading to misleading interpretations when only homogeneous null models are considered (Baddeley *et al.,* 2015; Diggle, 2013).

Although showing that STPP analysis using the mark variogram yields interesting results, Stoyan *et al.* (2017) do not justify their choice of the Gaussian model or discuss implications of using other valid models like spherical or exponential. In this article, we aimed only to complement the methodology by adding simulation envelopes, so since model selection was not our focus, this discussion was not included, leaving it for future work.

4. Conclusions

The analysis of an STPP using the variograms $\gamma_{sp}(r)$ and $\gamma_{te}(t)$, together with simulation envelopes, complements the approach proposed by Stoyan *et al.* (2017) by allowing formal assessment of whether observed patterns are compatible with homogeneous or non-homogeneous Poisson process assumptions.

Applying these methods to fire hotspot data proved effective for identifying spatiotemporal patterns and, mainly, for distinguishing apparent clustering caused by non-homogeneous intensity variation from genuine second-order dependence between events. The comparison between HPP- and NHPP-based simulation envelopes showed that part of the observed clustering behavior can be explained by first-order intensity effects rather than by interaction between fire hotspots. Thus, the proposed approach contributes to a more reliable interpretation of spatiotemporal clustering patterns and to a better understanding of fire dynamics in ecosystems such as the Brazilian Amazon rainforest.

Acknowledgments

This work was supported by the CAPES - Coordenação de Aperfeiçoamento de Pessoal de Nível Superior.

Conflicts of Interest

The authors declare no conflict of interest.

Author Contributions

Conceptualization: ABREU, R. F.; SCALON, J. D. **Data curation**: ABREU, R. F. **Formal analysis**: ABREU, R. F. **Investigation**: ABREU, R. F.; SCALON, J. D. **Methodology**: ABREU, R. F.; SCALON, J. D. **Software**: ABREU, R. F. **Resources**: ABREU, R. F.; SCALON, J. D. **Supervision**: ABREU, R. F.; SCALON, J. D. **Validation**:ABREU, R. F.; SCALON, J. D. **Visualization**: ABREU, R. F.; SCALON, J. D. **Writing – original draft**: ABREU, R. F.; SCALON, J. D. **Writing – review and editing**: ABREU, R. F.; SCALON, J. D.

References

1. Aragó, P, Juan, P, Díaz-Avalos, C & Salvador, P. Spatial point process modeling applied to the assessment of risk factors associated with forest wildfires incidence in Castellón, Spain. *European journal of forest research* **135,** 451–464. https://doi.org/10.1007/s10342-016-0945-z (2016).
2. Baddeley, A., Rubak, E. & Turner, R. *Spatial point patterns: methodology and applications with R* https://doi.org/10.1201/b19708 (Chapman and Hall/CRC, 2015).
3. Baddeley, A. & Turner, R. spatstat: An R Package for Analyzing Spatial Point Patterns. *Journal of Statistical Software* **12,** 1–42. https://doi.org/10.18637/jss.v012.i06 (2005).
4. Barbosa, R. I. *Savanas da Amazônia: emissão de gases do efeito estufa e material particulado pela queima e decomposição da biomassa acima do solo, sem a troca do uso da terra, em Roraima, Brasil* PhD thesis (Instituto Nacional de Pesquisas da Amazônia, 2001).
5. Beisbart, C. & Kerscher, M. Luminosity-and morphology-dependent clustering of galaxies. *The Astrophysical Journal* **545,** 6. https://doi.org/10.1086/317788 (2000).
6. Berman, M. & Diggle, P. Estimating Weighted Integrals of the Second-Order Intensity of a Spatial Point Process. *Journal of the Royal Statistical Society: Series B (Methodological)* **51,** 81–92. https://doi.org/10.1111/j.2517-6161.1989.tb01750.x (1989).
7. Brasil. Ministério da Agricultura, Pecuária e Abastecimento. Serviço Florestal Brasileiro. *Floresta Nacional do Jamari (RO)* Brasil. Ministério da Agricultura, Pecuária e Abastecimento. Serviço Florestal Brasileiro. https://www.gov.br/florestal/pt-br/assuntos/concessoes-e-monitoramento/concessoes-florestais-em-andamento/floresta-nacional-do-jamari-ro-2/floresta-nacional-do-jamari-ro-1.
8. Camargo, E. C. G., Fucks, S. D. & Câmara, G. Análise espacial de superfícies. *Análise espacial de dados geográficos. Planaltina: Embrapa Cerrados,* 79–122 (2004).
9. Chiu, S. N., Stoyan, D., Kendall, W. S. & Mecke, J. *Stochastic geometry and its applications* https://doi.org/10.1002/9781118658222 (John Wiley & Sons, 2013).
10. Comas, C. & Mateu, J. Modelling forest dynamics: a perspective from point process methods. *Biometrical Journal: Journal of Mathematical Methods in Biosciences* **49,** 176–196. https://doi.org/10.1002/bimj.200510268 (2007).
11. Corrêa, S. d. C. *A influência dos sistemas climáticos sobre os incêndios florestais: estudo de caso: evento de incêndio ocorrido em setembro de 2005 no Jardim Botânico de Brasília* PhD thesis (Universidade de Brasília, 2007).
12. Cressie, N. *Statistics for Spatial Data (Wiley Series in Probability and Statistics)* Revised Edition. https://doi.org/10.1002/9781119115151 (Wiley-Interscience, 1993).

13. Daley, D. J. & Vere-Jones, D. *An introduction to the theory of point processes* 2nd ed. https://doi.org/10.1007/b97277 (Springer, 2002).

14. Diggle, P. A kernel method for smoothing point process data. *Applied statistics,* 138–147. https://doi.org/10.2307/2347366 (1985).

15. Diggle, P. J. *Statistical analysis of spatial and spatio-temporal point patterns* https://doi.org/10.1201/b15326 (Chapman and Hall/CRC, 2013).

16. Diggle, P. J., Chetwynd, A. G., Häggkvist, R. & Morris, S. E. Second-order analysis of space-time clustering. *Statistical methods in medical research* **4,** 124–136. https://doi.org/10.1177/096228029500400203 (1995).

17. Diggle, P. J. & Gabriel, E. in *Handbook of Spatial Statistics* (eds Gelfand, A. E., Diggle, P. J., Fuentes, M. & Guttorp, P.) 449–461 (Chapman and Hall/CRC, London, 2010). https://doi.org/10.1201/9781420072884.

18. Gabriel, E. & Diggle, P. J. Second-order analysis of inhomogeneous spatio-temporal point process data. *Statistica Neerlandica* **63,** 43–51. https://doi.org/10.1111/j.1467-9574.2008.00407.x (2009).

19. Gabriel, E., Diggle, P. J., Rowlingson, B. & Rodriguez-Cortes, F. J. *stpp: Space-Time Point Pattern Simulation, Visualisation and Analysis* R package version 2.0-8 (2024). https://CRAN.R-project.org/package=stpp.

20. Gabriel, E., Rowlingson, B., Diggle, P, *et al.* stpp: an R package for plotting, simulating and analyzing Spatio-Temporal Point Patterns. *Journal of Statistical Software* **53,** 1–29. https://doi.org/10.18637/jss.v053.i02 (2013).

21. Gervini, D. Independent component models for replicated point processes. *Spatial Statistics* **18,** 474–488. https://doi.org/10.1016/j.spasta.2016.09.006 (2016).

22. ICMBio. *Mais de 90% dos incêndios têm ação humana, diz PrevFogo* Instituto Chico Mendes de Conservação da Biodiversidade, Brasília - DF: ICMBio, 2016. https://www.icmbio.gov.br/portal/ultimas-noticias/20-geral/8327-mais-de-90-dos-incendios-tem-acao-humana-diz-prevfogo.

23. Illian, J., Penttinen, A., Stoyan, H. & Stoyan, D. *Statistical analysis and modelling of spatial point patterns* https://doi.org/10.1002/9780470725160 (John Wiley & Sons, 2008).

24. INPE. *Programa Queimadas* INPE. https://terrabrasilis.dpi.inpe.br/queimadas/bdqueimadas.

25. Lawson, A. & Zhou, H. Spatial statistical modeling of disease outbreaks with particular reference to the UK foot and mouth disease (FMD) epidemic of 2001. *Preventive veterinary medicine* **71,** 141–156. https://doi.org/10.1016/j.prevetmed.2005.07.002 (2005).

26. Lloyd, C. D. *Local models for spatial analysis* https://doi.org/10.1201/EBK1439829196 (CRC press, 2010).

27. Mohler, G. O., Short, M. B., Brantingham, P. J., Schoenberg, F. P. & Tita, G. E. Self-exciting point process modeling of crime. *Journal of the American Statistical Association* **106,** 100–108. https://doi.org/10.1198/jasa.2011.ap09546 (2011).

28. Møller, J. & Díaz-Avalos, C. Structured spatio-temporal shot-noise Cox point process models, with a view to modelling forest fires. *Scandinavian Journal of Statistics* **37,** 2–25. https://doi.org/10.1111/j.1467-9469.2009.00670.x (2010).

29. Montero, J.-M., Fernández-Avilés, G. & Mateu, J. *Spatial and spatio-temporal geostatistical modeling and kriging* https://doi.org/10.1002/9781118762387 (John Wiley & Sons, 2015).

30. Nepstad, D. *et al.* Inhibition of Amazon deforestation and fire by parks and indigenous lands. *Conservation biology* **20,** 65–73. https://doi.org/10.1111/j.1523-1739.2006.00351.x (2006).

31. Ogata, Y. Space-time point-process models for earthquake occurrences. *Annals of the Institute of Statistical Mathematics* **50,** 379–402. https://doi.org/10.1023/A:1003403601725 (1998).
32. Olinda, S. Métodos de Monte Carlo para processos pontuais marcados. *Revista Brasileira de Biometria* **29,** 39–56 (2010).
33. Pawlas, Z. Empirical distributions in marked point processes. *Stochastic Processes and their Applications* **119,** 4194–4209. https://doi.org/10.1016/j.spa.2009.10.002 (2009).
34. Penttinen, A., Stoyan, D. & Henttonen, H. M. Marked point processes in forest statistics. *Forest science* **38,** 806–824. https://doi.org/10.1093/forestscience/38.4.806 (1992).
35. Perez, A. M., Ward, M. P. & Carpenter, T. E. Control of a foot-and-mouth disease epidemic in Argentina. *Preventive veterinary medicine* **65,** 217–226. https://doi.org/10.1016/j.prevetmed.2004.08.002 (2004).
36. Podur, J., Martell, D. L. & Csillag, F. Spatial patterns of lightning-caused forest fires in Ontario, 1976–1998. *Ecological Modelling* **164,** 1–20. https://doi.org/10.1016/S0304-3800(02)00386-1 (2003).
37. R Core Team. *R: A Language and Environment for Statistical Computing* R Foundation for Statistical Computing (Vienna, Austria, 2024). https://www.R-project.org/.
38. Ramos, R. M., Fonseca, R. L. & Morello, T. F. Unidades de conservação e proteção contra incêndios florestais: relação entre focos de calor e ações articuladas pelas brigadas contratadas. *Biodiversidade Brasileira* **6,** 135–148. https://doi.org/10.37002/biodiversidadebrasileira.v6i2.558 (2016).
39. Ribeiro Jr, P. J. & Diggle, P. *geoR: Analysis of Geostatistical Data* R package version 1.9-5 (2025). https://CRAN.R-project.org/package=geoR.
40. Scalon, J. Análise de dados espaciais com aplicações em R (2025).
41. Schoenberg, F. P. Multidimensional residual analysis of point process models for earthquake occurrences. *Journal of the American Statistical Association* **98,** 789–795. https://doi.org/10.1198/016214503000000710 (2003).
42. Snyder, D. L. & Miller, M. I. *Random Point Processes in Time and Space* 2nd ed. ISBN: 978-1-4612-7821-4,978-1-4612-3166-0. https://doi.org/10.1007/978-1-4612-3166-0 (Springer-Verlag New York, 1991).
43. Stoyan, D. & Penttinen, A. Recent applications of point process methods in forestry statistics. *Statistical Science,* 61–78. https://doi.org/10.1214/ss/1009212674 (2000).
44. Stoyan, D., Rodríguez-Cortés, F. J., Mateu, J. & Gille, W. Mark variograms for spatio-temporal point processes. *Spatial statistics* **20,** 125–147. https://doi.org/10.1016/j.spasta.2017.02.006 (2017).
45. Stoyan, D. & Wälder, O. On variograms in point process statistics, II: models of markings and ecological interpretation. *Biometrical Journal: Journal of Mathematical Methods in Biosciences* **42,** 171–187. https://doi.org/10.1002/(SICI)1521-4036(200005)42:2<171::AID-BIMJ171>3.0.CO;2-L (2000).
46. Turner, R. Point patterns of forest fire locations. *Environmental and ecological statistics* **16,** 197–223. https://doi.org/10.1007/s10651-007-0085-1 (2009).
47. Vere-Jones, D & Deng, Y. A point process analysis of historical earthquakes from North China. *Earthquake Research in China* **2,** 165–181 (1988).
48. Wälder, K. & Wälder, O. Analysing interaction effects in forests using the mark correlation function. *iForest-Biogeosciences and Forestry* **1,** 34. https://doi.org/10.3832/ifor0449-0010034 (2008).

49. Wälder, O. & Stoyan, D. On variograms in point process statistics. *Biometrical Journal* **38,** 895–905. https://doi.org/10.1002/bimj.4710380802 (1996).

50. Wiegand, T. & Moloney, K. A. *Handbook of spatial point-pattern analysis in ecology* https://doi.org/10.1201/b16195 (CRC press, 2013).

51. Zhang, T. & Zhuang, Q. On the local odds ratio between points and marks in marked point processes. *Spatial Statistics* **9,** 20–37. https://doi.org/10.1016/j.spasta.2013.12.002 (2014).